Journal of Molecular Spectroscopy 341 (2017) 1–9

Contents lists available at ScienceDirect

Journal of Molecular Spectroscopy

journal homepage: www.elsevier.com/locate/jms

High energy Rydberg and valence states and state interactions of DCl: New observations by mass resolved REMPI

Arnar Hafliðason, Huasheng Wang, Ágúst Kvaran *

Science Institute, University of Iceland, Dunhagi 3, 107 Reykjavík, Iceland

ARTICLE INFO

Article history:
Received 12 July 2017
In revised form 21 August 2017
Accepted 4 September 2017
Available online 12 September 2017

ABSTRACT

Mass resolved resonance enhanced multiphoton ionization (REMPI) spectra of a mixture of DCl and HCl were recorded for two-photon resonance excitation in the region of 80 500–89 500 cm^{-1}. Spectra due to resonance transitions to rovibrational states of number of Rydberg and ion-pair states of DCl, were identified and assigned. Five new spectral bands due to transitions to Rydberg states and eight new bands due to transitions to vibrational states of the ion-pair state were identified and analysed to derive energetic parameters. Irregularities observed in vibrational energy level spacing, rotational constants and isotope shifts of chlorine isotopologues from what to expect for unperturbed states, as well as relative signal intensities, are indicative of strong homogeneous interaction between the $E^1\Sigma^+$ Rydberg state and the $V^1\Sigma^+$ ion-pair state. These observations are found to be due to level-to-level interaction between E and V rovibrational states of same J' quantum numbers. Comparison of the data for DCl and HCl is performed.

1. Introduction

UV–Vis molecular spectroscopy and photofragmentation studies, presented in the literature, are largely associated with photoexcitations in a relatively low energy valence state region. Corresponding studies relevant to excitation to higher energy region of Rydberg states or mixed Rydberg and valence states are much fewer. Partly, this is due to a larger density of states and state mixing within molecules, which adds to the complexity of spectroscopic and photofragmentation analysis. Nevertheless, photoexcitation to the higher energy region of molecules are of great relevance to number of intriguing research fields such as atmospheric chemistry, astrochemistry, photosynthesis and plasma physics.

The simplicity of the diatomic hydrogen halides makes them ideal candidates for such fundamental studies. Relatively well resolved rotational spectral structures for excitations to high energy Rydberg and ion-pair (valence) states has allowed detailed quantum energy level based studies of spectroscopy [1–27] and photofragmentation [5,7,9–11,13,15–22,28–34] processes. Spectroscopic information have been sought by means of standard spectroscopy methods [1–3,24,28,35–40] as well as by REMPI [4–6,8–10,12–14,16–23,26,27,29,41–43] to characterize the energetics of large number of Rydberg states and ion-pair vibrational states. The use of varying number of photons for resonance excitations has proved to be useful in the search for, and characterization of, states. Spectral perturbations, showing as spectra line shifts or intensity alterations, are frequently observed. These have been taken account of by deperturbation calculations [18,20,21,31,44] and made use of to predict the energetics of hidden (or dark) states [26] as well as to determine state interaction strengths and properties [15–17,19,20,22,26] and to characterize dissociation processes [12,13,21,22]. Additionally, ion velocity map imaging studies, coupled with REMPI, have been used successfully to characterize photofragmentation (both photodissociation and photoionization) and excitation processes involved [21,22,44–47]. Furthermore, the methodology of *ab initio* calculations, relevant to electronically excited molecular states, has gained from an association with the experimental work and proved to be useful as a guiding tool in data interpretations [48–56].

Largest amount of data has been collected for HCl [1,4–6,10,11,29,31,35,39,41,42,57,58], whereas a lot less data are available for its deuterated counterpart, DCl. The early work on the absorption spectroscopy of DCl by Tilford and Ginter in 1971 [35] and by Douglas and Greening in 1979 [3], resulted in discovery of a number of Rydberg states and medium high energy vibrational states of the $V^1\Sigma$ ion-pair state. Later, Callaghan et al. [23] published work on $(2+n)$ REMPI of HCl and DCl. Coxon et al., [24] observed the lowest vibrational bands of the $V^1\Sigma^+$ state by emission spectroscopy. Vibrational bands of the $V^1\Sigma^+$ ion-pair state for $v' = 8–11$ and from $v' = 22$ upwards, for DCl, are yet to be observed.

* Corresponding author.
E-mail address: agust@hi.is (Á. Kvaran).

http://dx.doi.org/10.1016/j.jms.2017.09.002
0022-2852/

More recently, through (3 + 1) REMPI, Kvaran et al. reported previously unobserved Rydberg states, for HCl and DCl [11,58]. No data, relevant to the dynamics or photofragmentation of DCl involving states in this high energy region, are available in the literature. Whereas theoretical interpretation of high energy state interaction has been performed for HCl [48], no such work is available for DCl.

In this paper we present (2 + n) REMPI data and analysis for the two-photon resonance excitation region of 80500–89500 cm^{-1} for a mixture of DCl and HCl. Number of new spectral observations, for DCl, are assigned, including previously unobserved vibrational bands of the $V^1\Sigma^+$ ion-pair state and for Rydberg states. Detailed analysis of the data involve standard spectral structure fit analysis and/or simulation calculations. A special attention is paid to perturbation effects which appear as deviation of spacings between vibrational energy levels, rotational constants and chlorine isotope shifts from regular patterns of unperturbed states/Morse potentials. The analysis lead to quantitative characterization of states and reveal a characteristic pattern of strong interactions between singlet sigma states, indicating a diversity in dynamical processes in this high energy region. Comparison of data for DCl and HCl is performed.

2. Experimental

DCl was produced by a reaction of benzoyl chloride and deuterated water to give a mixture of DCl and HCl in a ratio of about 60:40 ratio [59]. The product was transferred to and stored in a gas cylinder. Mass resolved REMPI spectra were recorded for the mixture of HCl and DCl diluted in argon (HCl/DCl 50%, Argon 50%) after a jet expansion of the mixture through a pulsed nozzle to form a molecular beam. The apparatus used has been described before [58,60,61]. Equipment and condition parameters are listed in Table 1. Excitation radiation was generated with a Lambda Physik COMPex 205 excimer laser (XeCl, 308 nm) pumped Coherent ScanMatePro dye laser followed by a frequency doubling by a BBO crystal. The laser beam was focused on the molecular beam by a 200 mm quartz focal lens between a repeller and extractor plates. Ions produced were directed into a 70 cm time-of-flight tube and detected by MCP detector plates. Signals were fed into a LeCroy WaveSurfer 44 MXs-A, 400 MHz storage oscilloscope and recorded as mass spectra vs. laser excitation wavenumber. To prevent saturation effects and power broadening, laser power was minimized. Calibration was based on known spectral peaks of the major HCl REMPI signals [4]. Accuracy was found to be about ±1.0 cm^{-1} on the two-photon wavenumber scale.

Table 1
Typical equipment and condition parameters for REMPI experiments.

(a)	HCl/DCl/Ar sample	About (DCl 60%: HCl 40%) 50%: argon 50%
(b)	Laser dyes	C-440, C-460 & C-480
(c)	Freq. doubling crystal	Sirah BBO-2
(d)	Laser repetition rate	10 Hz
(e)	Dye laser linewidth	0.095 cm^{-1}
(f)	Laser intensity used	10–16 mJ/pulse from Dye laser, 0.5–1.0 mJ after SHG
(g)	Nozzle size	0.5 mm
(h)	Sample backing pressure	2–3 bar
(i)	Pressure inside ion chamber	$5{\cdot}10^{-7}$ mbar
(j)	Nozzle opening time	180–250 μs
(k)	Delay time for laser excitation	450–500 μs
(l)	Excitation step size	0.1 cm^{-1}
(m)	Time-Of-Flight step size	10 ns
(n)	Time-Of-Flight tube length	70 cm
(o)	Focal lens distance	200 mm

3. Results and analysis

Ion yields as a function of two-photon wavenumber excitation (mass resolved REMPI spectra) were derived for all observed ions formed by REMPI of H^iCl and D^iCl; i = 35, 37 (see Table 2), for the excitation region of 80500–89500 cm^{-1}. Signals due to (2 + n) REMPI of D^iCl, for both i = 35 and 37 were used to assign spectra and to characterize vibrational states of electronically excited $D^{35}Cl$ and to derive isotope shifts for the two isotopologues D^iCl; i = 35, 37, whereas those due to REMPI of known $H^{35}Cl$ states [4–6] were used for wavelength calibration. Fig. 1a–c shows D^iCl REMPI spectra for two-photon resonance transitions to the Rydberg states $E^1\Sigma^+(0^+)$ ($v' = 0$) (a) and $I^1\Delta_2(v' = 0)$ (c) and to the valence/ion-pair state $V^1\Sigma^+(0^+)(v' = 22)$ (b). More spectra, relevant to the analysis of $D^{35}Cl$, are to be found in Supplementary material [62]. In agreement with observations for H^iCl [10,15,18,30,34] the $\Omega = 0$ Rydberg states (the $E^1\Sigma^+$ state in particular) and the ion-pair state spectra show relatively large signals for both the fragment and parent molecular ions (dominating 1a and 1b), whereas, those of Rydberg states for $\Omega > 0$ and triplet states show dominating parent molecular ion signals (Fig. 1c). The former observation is believed to indicate large mixing of the $\Omega = 0$ Rydberg and ion-pair states due to strong homogeneous interactions [23,24,33–35]. $D^{35}Cl$ spectra due to resonance transitions to Rydberg states were either analysed by use of the PGOPHER simulation program [63], or by fitting analytical expressions for peak positions as a function of quantum numbers of the energy levels involved [9,12,18,62], to give rotational parameters (B', D') and band origins (ν^0) for given rotational constants for the ground state [64] (see Table 3). Most $D^{35}Cl$ spectra, previously detected in this excitation region, were identified and assigned. In addition, several new spectral bands and/or new rotational lines were observed and assigned (see Table 3 and Ref. [62]). These will now be dealt with in more detail. Shorter abbreviations for the Rydberg and ion-pair vibrational states involved will be frequently used, e.g., $V(17)$ for $V^1\Sigma^+(v' = 17)$ and $E(0)$ for $E^1\Sigma^+(v' = 0)$.

3.1. Spectra due to two-photon resonance transitions to Rydberg states

Number of Rydberg state spectra, previously assigned [3,23,35] were identified [62] and analysed to give spectroscopic parameters of good agreement with values derived before (Table 3). In addition five new bands (unreported) were observed:

A new band was observed in the two-photon wavenumber region of 88200–88280 cm^{-1} showing weak Q, R and S lines (Fig. 2a) [62]. Only signals due to the parent molecular ion, DCl^+ were observed, which is typical for an excited state of negligible mixing with the $V^1\Sigma^+$ ion-pair state [15–20,22,30,34,65]. Spectroscopic parameters for $D^{35}Cl$, evaluated from analysis of the spectra are listed in Table 3. Chlorine isotope shift ($\Delta\nu^0(35, 37)$ for ^iCl; i = 35, 37 [66,67]) of about 8 cm^{-1} was obtained. The values of the band origin (ν^0), rotational constant ($B_{v'}$) and isotope shift ($\Delta\nu^0(35, 37)$) are logical continuation of the corresponding values

Table 2
Ions formations in REMPI of H^iCl and D^iCl; i = 35, 37.

Mass numbers/amu	Parent molecules/ions formed		
	H^iCl	H^iCl/D^iCl	D^iCl
1	H^+		
2			D^+
35		$^{35}Cl^+$	
36	$H^{35}Cl^+$		
37		$^{37}Cl^+$	$D^{35}Cl^+$
38	$H^{37}Cl^+$		
39			$D^{37}Cl^+$

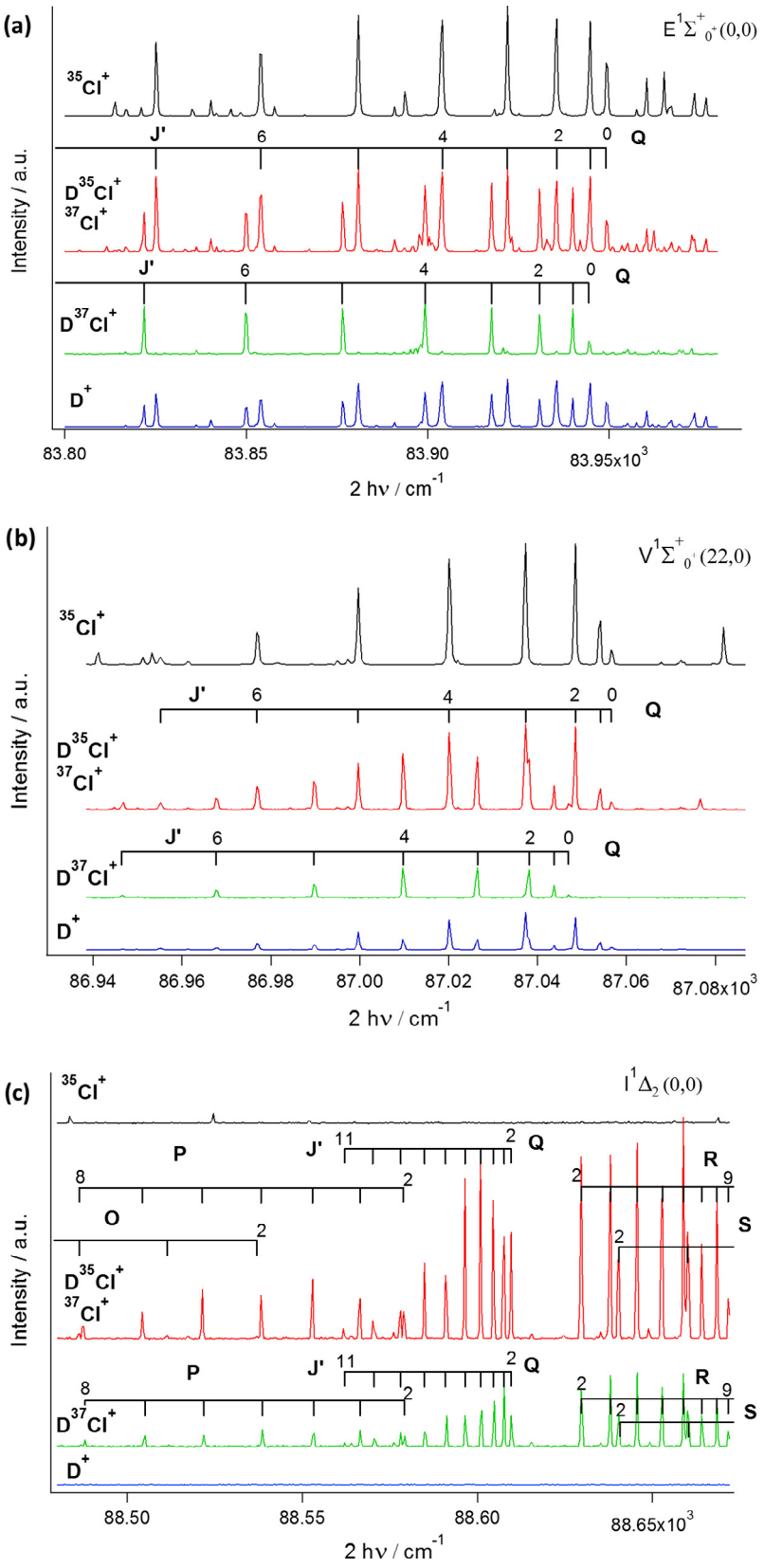

Fig. 1. REMPI spectra of mixtures of D^{i}Cl(g) and H^{i}Cl(g); i = 35, 37 for the ions $^{35}Cl^+$ (mass 35; black), $D^{35}Cl^+$ and $^{37}Cl^+$ (37; red), $D^{37}Cl^+$ (39; green) and D^+ (2; blue) (see Table 2). *J'*-quantum numbers for the excited states of rotational peaks corresponding to two-photon resonance excitation from the ground state to the $E^1\Sigma^+(v' = 0)$ (*Q* lines) (a), $V^1\Sigma^+(v' = 22)$ (*Q* lines) (b) and $I^1\Delta_2(v' = 0)$ (*O, P, Q, R, S* lines) (c) of $D^{35}Cl$ and $D^{37}Cl$ are indicated. (For interpretation of the references to colour in this figure legend, the reader is referred to the web version of this article.)

Table 3
Vibrational (band origins and spacing between v′ levels) and rotational parameters (B' and D') for (a) ion-pair and (b) Rydberg states of $D^{35}Cl$.

State	v′	ν^0/cm^{-1}		B'/cm^{-1}		D'/cm^{-1}	
		Our work	Others' work	Our work	Others' work	Our work	Others' work
(a) Rydberg states							
$E^1\Sigma^+$	0	83949.4	83944[a]	3.181	3.0	0.0004	
	1	85014		3.19		−0.0021	
	2	86823.8	86812[a]	3.40	3.7	0.0007	
	3	88667		3.58		0.01435	
$H^1\Sigma^+$	0	88689.1	88694[c]	4.620	4.658	0.00038	0.00095
$D^1\Pi_1$	0	82528.0	82525.8[b]	5.039	5.077	0.00015	0.00028
$F^1\Delta_2$	0	82908.8	82907[a]	5.136	5.195	0.00003	0.0002
	1	84737.0	84735[a]	5.043	5.447	0.00005	0.0028
	2	86511.3	86504[a]	4.928	4.934	0.00002	0.0004
	3	88227.2		4.820		0.00005	
$I^1\Delta_2$	0	88611.8		5.021		0.00015	
$d^3\Pi_1$	0	81787.5	81784[a]	5.286	5.167	0.0026	
$f^3\Delta_2$	0	82076.6	82074.2[b]	5.301	5.329	0.00031	0.00039
$f^3\Delta_1$	0	82561.0		5.115		−0.00032	
$i^3\Delta_2$	0	87678.1		5.084		0.00011	
$g^3\Sigma^-$	0	83133.6	83131[a]	4.381	4.40	−0.0013	
$j^3\Sigma^-$	0	89286.3	89287.6[c]	5.120	5.080	0.0005	0.0057
(b) $V^1\Sigma_g^+$ ion-pair vibrational states							
$V^1\Sigma^+$	11	82494	82582[a]	(2.916)[d]	3		0.0099
	12	82943	82942[c]	1.792	1.822	0.0013	0.0018
	13	83390	83389[c]	1.941	2.198	−0.0047	0.0111
	14	83738	83734[a]	2.965	3.0	0.0056	
	15	84297	84294[a]	2.208	2.1	−0.0005	
	16	84666	84660[a]	2.342	2.3	0.0010	
	17	84950	84948[a]	3.417	3.1	0.0049	
	18	85478	85474[a]	2.590	2.3	0.0006	
	19	85844	85838[a]	2.049	2.1	−0.0014	
	20	86217	86217[a]	2.224	2.4	0.0015	
	21	86588	86580[a]	2.408	2.3	0.0056	
	22	87053		2.637		−0.0074	
	23	87417		2.102		0.0007	
	24	87804		1.736		−0.0017	
	25	88173		2.222		0.0043	
	26	88475		2.233		0.0039	
	27	88978		1.630		−0.0082	
	28	89242		2.653		−0.0105	

[a] Ref. [23].
[b] Ref. [35].
[c] Ref. [3].
[d] The B' value for $v'(V) = 11$ is "abnormally" high, which could be due to a near-degenerate interaction between the $D^1\Pi_1(v' = 0)$ and $V(11)$ states for low J' levels.

for the v′ = 0–2 states of the $F^1\Delta_2$ Rydberg state for the v′ = 3 state (see Table 3 for ν^0 and B_v; ^{i}Cl isotope shifts of 0.4 cm^{-1}, 2.4 cm^{-1} and 5.2 cm^{-1} were derived for the v′ = 0, 1 and 2 spectra, respectively). We, therefore, assign the spectrum at $\nu^0 = 88227.2$ cm^{-1} to the $F^1\Delta_2$ (v′ = 3), $(\sigma^2\pi^3)4p\pi$ Rydberg state. Assuming a Morse potential and the relationship $B_v = B_e - \alpha_e(v' + ½)$ to hold [68] values of $T_e = 81973.3$ cm^{-1}, $\omega_e = 1885.1$ cm^{-1}, $\omega_e x_e = 28.075$ cm^{-1}, $B_e = 5.199$ cm^{-1} and $\alpha_e = 0.1083$ cm^{-1} were derived for the $F^1\Delta_2$ electronic state of $D^{35}Cl$.

A relatively strong band, with a clear structure of *O, P, Q, R* and *S* lines for a Δ Ω = 2 (ΔΛ = 2) two-photon transition (i.e. $\Delta_2 \leftarrow\leftarrow \Sigma$), was observed in the region of 88350–88810 cm^{-1} (Fig. 2b). Only signals due to the parent molecular ion, DCl^+ were observed (see also Fig. 1c for comparison). Evaluated spectroscopic parameters are listed in Table 3. The band origin is +29.4 cm^{-1} higher than that of the $I^1\Delta_2$ (v′ = 0) state spectrum for $H^{35}Cl$ [4], typical for a hydrogen isotope shift ($\Delta\nu^0(1, 2)$) for a v′ = 0 Rydberg state. We assign the spectrum at $\nu^0 = 88611.8$ cm^{-1} to the $I^1\Delta_2$ (v′ = 0), $(\sigma^2\pi^3)3d\pi$ Rydberg state.

A relatively strong band, also with a clear structure of *O, P, Q, R* and *S* lines for a Δ Ω = 2 (ΔΛ = 2) two-photon transition, was observed in the region of 87500–87850 cm^{-1} (Fig. 2c). Only signals due to the parent molecular ion, DCl^+ were observed. Evaluated spectroscopic parameters are listed in Table 3. The band origin is +21.1 cm^{-1} higher than that of the $i^3\Delta_2$ (v′ = 0) state spectrum for $H^{35}Cl$ [4]. We, therefore, assign the spectrum at $\nu^0 = 87678.1$ cm^{-1} to the $i^3\Delta_2$ (v′ = 0), $(\sigma^2\pi^3)3d\pi$ Rydberg state.

A new band was observed in the two-photon wavenumber region of 84790–85000 cm^{-1} showing only weak *Q* lines analogous to that found for *E*(0) (see Fig. 1a) [62]. Signals due to the parent molecular ion, DCl^+ and to a lesser extent, the fragment ions, D^+ and Cl^+ were observed, which is typical for a mixing of the Rydberg state with the $V^1\Sigma^+$ ion-pair state due to a strong homogeneous (Δ Ω = 0) interaction [10,15,16,18–20,30]. Assuming the lowest J' level peak, observed, to be $J' = 3$, the spectroscopic parameters listed in Table 3 were derived. The proximity of the $V^1\Sigma^+(v' = 17)$ state ($\nu^0 = 84950$ cm^{-1}; $\Delta\nu^0 = 64$ cm^{-1}) makes it a likely candidate for the strongly interacting state. An enhanced energy gap between the $V(v' = 17)$ and $V(v' = 18)$ states in the series of ion-pair vibrational states (see Fig. 3a and the section below) is a further indication of a homogeneous interaction analogous to that observed between the $E^1\Sigma^+(v')$ and $V^1\Sigma^+(v')$ states for HCl [10,15,18,69,70]. We, therefore, assign the spectrum at $\nu^0 = 85014$ cm^{-1} to the $E^1\Sigma^+(v' = 1)$, $(\sigma^2\pi^3)4p\pi$ Rydberg state.

A new, very weak band is observed in the two-photon wavenumber region of 88590–88670 cm^{-1} showing only weak *Q* lines (Fig. 2d) [62]. Both signals due to the parent molecular ion, DCl^+ and the fragment ion, Cl^+ are observed. Assuming the lowest J' level peak, observed, to be $J' = 1$, the spectroscopic parameters listed in Table 3 were derived. The proximity of the $V^1\Sigma^+(v' = 26)$

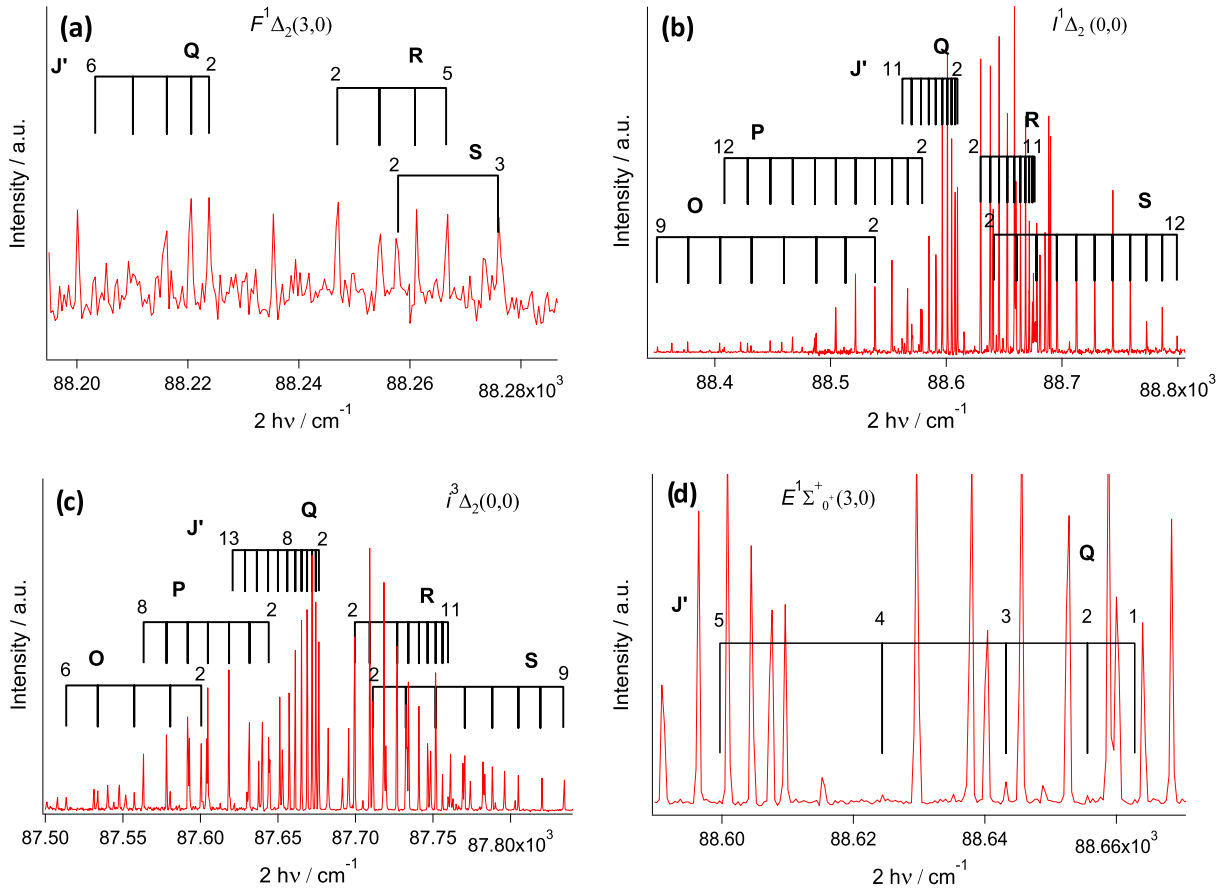

Fig. 2. REMPI spectra of mixtures of D^{i}Cl(g) and H^{i}Cl(g); i = 35, 37 for the ions D^{35}Cl$^+$ and ^{37}Cl$^+$ (mass 37) (see Table 2). *J'*-quantum numbers for the Rydberg excited states of rotational peaks corresponding to two-photon resonance excitation from the ground state to the $F^1\Delta_2$(v′ = 3) (*Q, R, S* lines) (a), $I^1\Delta_2$ (v′ = 0) (*O, P, Q, R, S* lines) (b), $i^3\Delta_2$(v′ = 0) (*O, P, Q, R, S* lines) (c) and $E^1\Sigma^+$(v′ = 3) (*Q* lines) (d) of D^{35}Cl are indicated.

state (ν^0 = 88 475 cm^{-1}; $\Delta\nu^0$ = 192 cm^{-1}) makes it a likely candidate for a strongly interacting state. An enhanced energy gap between the *V*(v′ = 26) and *V*(v′ = 27) states in the series of ion-pair vibrational states (see Fig. 3a and the section below) is a further indication of a homogeneous interaction. We, therefore, assign the spectrum at ν^0 = 88 667 cm^{-1} to the $E^1\Sigma^+$(v′ = 3), $(\sigma^2\pi^3)4p\pi$ Rydberg state.

3.2. Spectra due to two-photon resonance transitions to ion-pair states and state interactions

Signals of DCl$^+$ as well as D$^+$ and Cl$^+$ for *Q* lines, only, due to transitions to *V*(v′), previously detected in absorption (v′ = 12–21) [3] and REMPI (v′ = 14–21) [23,25] were identified (Fig. 1b) [62] and analysed to give spectroscopic parameters in good agreement with values derived before (Table 3). In addition analogous signals due to transitions to *V*(v′); v′ = 11, 22–28 were observed, assigned and analysed to give ν^0, $B_{v'}$ and $D_{v'}$ values for D^{35}Cl (Table 3). Fig. 3a–c shows the band origins for D^{35}Cl along with the corresponding energy levels for H^{35}Cl [4], and plots of the vibrational energy level spacings ($\Delta\nu^0$(v′ + 1, v′)) (a), values of $B_{v'}$ (b) and isotope shifts ($\Delta\nu^0$(35, 37)) (c) as a function of energy/v′ tilted to the right (DCl) and left (HCl). All the plots in Fig. 3a–c show irregular structures for high v′s of about v′ > 11 for DCl and v′ > 8 for HCl, for analogous energy thresholds in both cases. The irregularities in the $\Delta\nu^0$(v′ + 1, v′) (a) and $B_{v'}$ (b) values observed for HCl have been explained to be due to an interaction, repulsive in nature, between *E* and *V* rovibrational states of same *J′* quantum numbers [9]. This is according to a level-to-level interaction between states, which depends on the interaction strength ($W_{E,V}$) and the energy gap between the corresponding levels ($\Delta E_{E,V}(J') = E_E(J') - E_V(J')$), which results in a shift of the energy level for the *V* state ($\Delta E_V(J') = E_V(J') - E^0{}_V(J')$) according to [17,68],

$$\Delta E_V(J') = (1/2)(\Delta E_{E,V}(J') - ((\Delta E_{E,V}(J'))^2 - 4(W_{E,V})^2)^{1/2} \quad (1)$$

where E^0 and E are the unperturbed and perturbed energies, respectively.

Vibrational energy level spacing vs. v′ (Fig. 3a): The vibrational energy level spacing ($\Delta\nu^0$(v′ + 1, v′)) as a function of energy/v′ for *V* (v′(*V*)) in the case of v′(*V*) ≈ 1–12 for DCl is found to decrease almost linearly with v′(*V*) as to be expected for an unperturbed state/Morse potential [68]

$$\Delta\nu^0(\nu' + 1, \nu') = \omega_e - 2\omega_e x_e(\nu' + 1) \quad (2)$$

analogous to that found for HCl in the case of v′(*V*) ≈ 4–10. Irregularities, on the other hand, are observed for higher energies/v′(*V*) (see Fig. 3a). As for HCl the irregularities observed for DCl we believe to be mostly due to a homogeneous interaction between the $E^1\Sigma^+((\sigma^2\pi^3)4p\pi)$ Rydberg state and the $V^1\Sigma^+(\sigma^1\pi^4\sigma^{*1})$ ion-pair state, resulting in a repulsion of rovibrational energy levels with same *J′* quantum numbers, inversely proportional to the energy differences. This appears as shift of vibrational and rotational energy levels of the interacting states as well as the corresponding spectral lines [9,10]. Thus, enhanced energy gaps appear between v′(*V*) = 14 and 15, 17 and 18, 21 and 22 as well as 26 and 27 due to the interactions with the *E*(0), *E*(1), *E*(2) and *E*(3) states, respectively, analogous to those observed between v′(*V*)

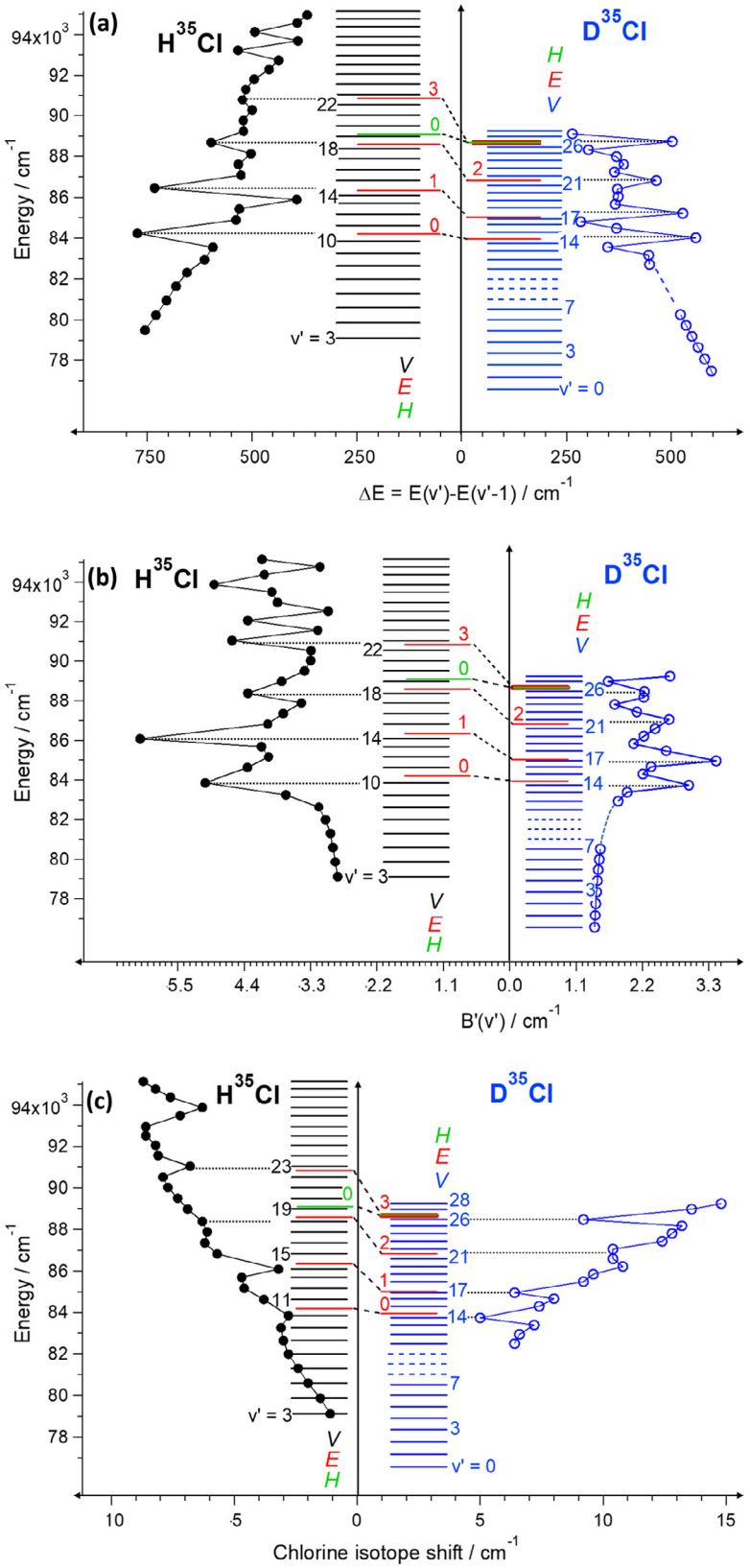

Fig. 3. $D^{35}Cl$ and $H^{35}Cl$: Vibrational energy levels for the $E^1\Sigma^+$ (red), $H^1\Sigma^+$ (green) and $V^1\Sigma^+$ (blue ($D^{35}Cl$); black ($H^{35}Cl$)) states as well as vibrational energy level spacing ($\Delta v^0(v'+1, v') = v^0(v'+1) - v^0(v')$; cm^{-1}) (a), rotational constants ($B_{v'}$) (b) and chlorine isotope shifts ($\Delta v^0(35, 37) = v^0(35; v', v''=0) - v^0(37; v', v''=0)$) (c) as a function of v' for the $V^1\Sigma^+$ states of $D^{35}Cl$ (blue curves tilted to the right) and $H^{35}Cl$ (black curves, tilted to the left). The energies (cm^{-1}; y-axis) are normalized to a zero value for the ground state $v''=0$ level for $D^{35}Cl$. Notice that the scales for $\Delta v^0(v'+1, v')$ (a), $B_{v'}$ (b) and $(\Delta v^0(35, 37)$ (c) are directed to left for HCl and to right for DCl. Values for HCl are derived from Ref. [4]. Values relevant to $v'(V) = 0$–7 for DCl are from Ref. [24]. Broken lines relevant to $v'(V) = 8$–10(11) (DCl) are guess values. Values relevant to $v'(V) = 11$–28 (DCl) are from this work. Levels for the Rydberg states of DCl are from this work. v'quantum numbers are indicated. (For interpretation of the references to colour in this figure legend, the reader is referred to the web version of this article.)

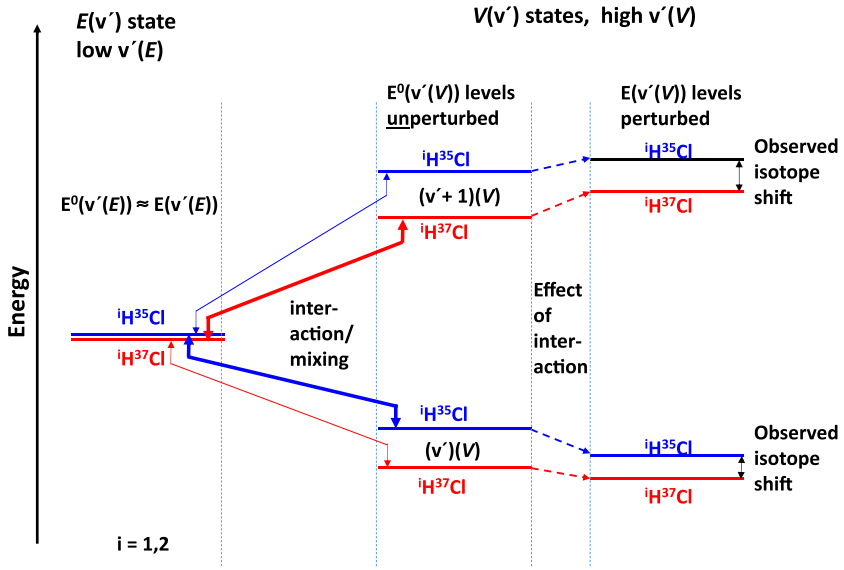

Fig. 4. Effect of interactions between $E(v')$ states and $V(v'+1)$ and $V(v')$ states on chlorine isotope shifts ($\Delta v^0(35, 37)$) for zero order energies (E^0) as, $E^0((v'+1)(V)) > E^0(v'(E)) > E^0(v'(V))$. $^iH^{35}Cl$ are in blue and $^iH^{37}Cl$ in red. Horizontal levels are energy levels, boldness of which indicates strength of mixing/repulsion effect. Double arrows represent repulsion interactions and single arrows represent effect of interactions. $v'(E)$ and $v'(V)/(v'+1)(V)$ are vibrational states of the E and V electronic states, respectively.

= 10 and 11, 14 and 15, 18 and 19 as well as 22 and 23 due to the interactions with the $E(v')$; $v' = 0$–3 states for HCl. It is worth noting that, by analogy to observations for HCl, corresponding interaction effects are believed to be negligible due to the $H^1\Sigma^+((\sigma^2\pi^3)3d\pi)$ Rydberg state (see Fig. 3a for $H(0)$).

Rotational constants vs. $v'(V)$ (Fig. 3b): Vibrational state rotational constants ($B_{v'}$) for an unperturbed electronic state/Morse potential are expected to decrease linearly with v' [68]

$$B_{v'} = B_e - \alpha_e(v' + 1) \tag{3}$$

However, the values for the low $v'(V)$ are found to increase gradually for $v'(V) = 0$–7 and to show irregularity as a function of $v'(V)$ for $v'(V) > 11$ (see Fig. 3b). Analogous effects are observed for HCl. The major effects, most likely, also are due to the above mentioned homogeneous interaction between the $E(v')$ and $V(v')$ states. Effectively it results in an expansion of the $V(v')$ states rotational levels and compression of those for the $E(v')$ states, hence an increase and decrease in the corresponding rotational constants, respectively [9,10]. This effect is inversely proportional to the energy differences between the interacting levels. Thus, the maxima in the $B_{v'}$ vs. $v'(V)$ plot for DCl for $v'(V) = 14$, 17, 22 and 26 (25) (see Fig. 3b) are indicative of the largest mixing of those vibrational states with $E(0)$, $E(1)$, $E(2)$ and $E(3)$, respectively. Lowering in the $B_{v'}$ values for the $v'(V)$ states on both sides (higher and lower in energy), as observed, is a consequence of a decreasing mixing with energy difference.

Chlorine isotope shift vs. $v'(V)$ (Fig. 3c): To a first approximation the chlorine isotope shift ($\Delta v^0(35, 37)$) for $^iH^{35}Cl$ and $^iH^{37}Cl$; i = 1, 2, is expected to increase linearly with v' for an unperturbed state/Morse potential [66,67]

$$\Delta n^0(35, 37) = v^0(35; v', v'' = 0) - v^0(37; v', v'' = 0); \tag{4a}$$

$$\Delta v^0(35, 37) \approx [\omega'_e(35)(v' + 1/2) - \omega'_e(35)(1/2)][1 - \rho(35, 37)] \tag{4b}$$

$$\rho(35, 37) = \sqrt{\mu_{37}/\mu_{35}} \tag{4c}$$

where $v^0(35; v', v'' = 0)$ and $v^0(37; v', v'' = 0)$ are the band origins for the two isotopologues, $\omega'_e(35)$ and $\omega''_e(35)$ are the vibrational frequencies (in cm^{-1}) of $^iH^{35}Cl$ for the excited and ground states, respectively. μ_{37} and μ_{37} are the reduced masses of the isotopologues. The plots of $\Delta v^0(35, 37)$ vs. $v'(V)$, both for DCl and HCl (Fig. 3c), however, show clear deviations from increasing linearities. Dips in the plots show close correlation with the corresponding observations (increases) for the vibrational energy level spacing ($\Delta v^0(v' + 1, v')$) (Fig. 3a) and rotational constants ($B_{v'}$) (Fig. 3b), which were interpreted as being due to the interactions with the $E(v')$ states above. Thus, for example, the lowering in the values of $\Delta v^0(35, 37)$ for $v'(V) = 14$, 17, 22(21) and 26 for DCl and of $v'(V) = 10$, 14, 18(17) and 23 for HCl match the enhanced values observed for $B_{v'}$. This can be explained to be due to a different degree of repulsion between $E(v')$ and $V(v')$ levels, for equal J' values ($\Delta E_{J'}$) for $D^{35}Cl$ ($H^{35}Cl$) and $D^{37}Cl(H^{37}Cl)$ levels associated with different spacing between the levels as shown in Fig. 4. Thus, a $v'(V)$ level of $^iH^{35}Cl$ (higher in energy than a $v'(V)$ level for $^iH^{37}Cl$), experiences larger downward energy shift than a $v'(V)$ level for $^iH^{37}Cl$ in the case when the $v'(V)$ levels are lower in energy than the interacting $v'(E)$ state, whereas a $(v' + 1)(V)$ level of $^iH^{35}Cl$, experiences less upwards energy shift than a $(v' + 1)(V)$ level for $^iH^{37}Cl$ in the case when the $v'(V)$ levels are higher in energy than the interacting $v'(E)$ state. In both cases this results in a lowering of the chlorine isotope shifts (see Fig. 3c).

4. Conclusion

Mass resolved REMPI spectra were recorded for a supersonic jet expansion of a mixture of $^iH^jCl(g)$; i = 1, 2; j = 35, 37 in argon for two-photon resonance excitation in the region of 80 500–89 500 cm^{-1}. Peaks due to resonance transitions from the ground states of D^jCl; j = 35, 37 to vibrational states of a number of Rydberg states and the ion-pair state, $V^1\Sigma^+$, depending on $J' \leftarrow\leftarrow J''$ transitions (line series) were identified and assigned. Spectral bands of the ion-pair states and the $E^1\Sigma^+$ states showed significant REMPI signals for both fragment ions (D^+, $^jCl^+$) and the parent molecular ions (D^jCl^+), whereas spectra of other Rydberg states showed very small or negligible fragment ion signals. The former is characteristic of an ion-pair character of the excited state, which, in the case of the E state is indicative of a large mixing of the E and V states due to strong homogeneous interaction. In addition to

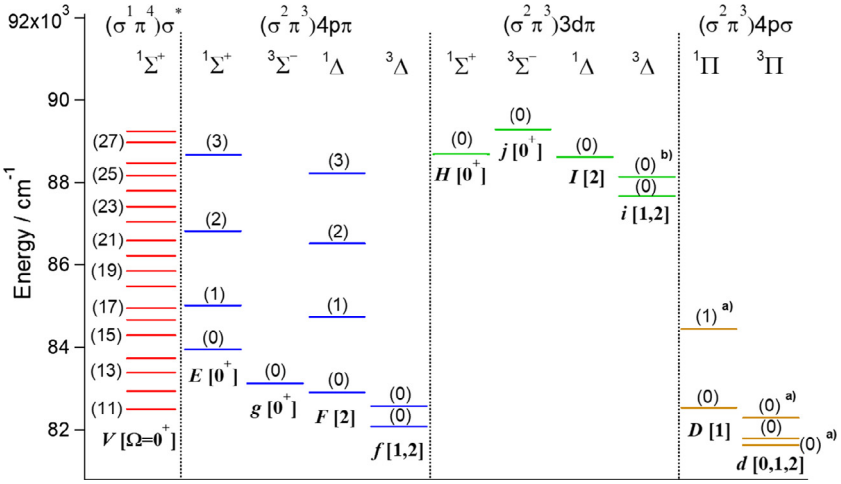

Fig. 5. Energy level diagram of known electronic states of $D^{35}Cl$ within the wavenumber range of 80 500–89 500 cm^{-1}. Vibrational quantum numbers are indicated inside brackets as (v′). Electronic states are labelled as $Y[\Omega', \ldots]$ for characteristic letters Y. Electron configurations and term symbols are shown on top. Levels are from this work except those marked by (a) (from Ref. [35]) and (b) (from Ref. [3]).

number of previously observed spectral bands, five new bands due to transitions to Rydberg states and eight new bands due to transitions to vibrational states of V were identified and analysed. Detailed analysis resulted in values of band origin (ν^0) and effective rotational constants ($B_{v'}$ and $D_{v'}$) for $D^{35}Cl$ (see Table 3). New Rydberg states, observed, were the $F^1\Delta_2$ (v′ = 3), $I^1\Delta_2$ (v′ = 0), $i^3\Delta_2$ (v′ = 0), $E^1\Sigma^+$(v′ = 1) and $E^1\Sigma^+$(v′ = 3) states. New vibrational states of V ($V^1\Sigma^+$(v′)), observed, were for v′ = 11, 22–28 (see Table 3 and summary Fig. 5).

The strong homogeneous interaction between the $E^1\Sigma^+$and $V^1\Sigma^+$(v′) states appears as perturbation effects (i.e. deviation of spectroscopic parameters from regular patterns of unperturbed states) in the DCl spectra analogous to what has been found for HCl to some extent: (A) Characteristic enhancement in energy gaps between neighbouring vibrational levels of the V state ($\Delta\nu^0$(v′ + 1, v′)) are observed for (v′ + 1) and v′ states higher and lower in energy than E(v′) levels (see Fig. 3a). (B) Enhancement in rotational constants ($B_{v'}$) were observed for V(v′) states closest in energy to neighbouring E(v′) states (see Fig. 3b). (C) Lowering in chlorine isotope shifts ($\Delta\nu^0$(35, 37)) were observed for V(v′) states closest in energy to neighbouring E(v′) states (see Fig. 3c). All these observations (A-C) can be explained to be due to level-to-level interaction between E and V rovibrational states of same J' quantum numbers, which appears as a repulsion between the corresponding energy levels.

The results of this paper adds to information relevant to the energetics, state interactions and fragmentation processes in the region of high energy Rydberg states of DCl. It will hopefully render further theoretical interpretation of the characteristic state interaction within the hydrogen halides [48].

Acknowledgements

The financial support of the University Research Fund, University of Iceland and an assistant teacher grant from University of Iceland for A.H. are gratefully acknowledged.

Appendix A. Supplementary material

Supplementary data associated with this article can be found, in the online version, at http://dx.doi.org/10.1016/j.jms.2017.09.002.

References

[1] S.G. Tilford, M.L. Ginter, J.T. Vanderslice, J. Mol. Spectrosc. 33 (1970) 505–519.
[2] S.G. Tilford, M.L. Ginter, A.M. Bass, J. Mol. Spectrosc. 34 (1970) 327.
[3] A.E. Douglas, F.R. Greening, Can. J. Phys. 57 (10) (1979) 1650–1661.
[4] D.S. Green, G.A. Bickel, S.C. Wallace, J. Mol. Spectrosc. 150 (2) (1991) 303–353.
[5] D.S. Green, G.A. Bickel, S.C. Wallace, J. Mol. Spectrosc. 150 (2) (1991) 354–387.
[6] D.S. Green, G.A. Bickel, S.C. Wallace, J. Mol. Spectrosc. 150 (2) (1991) 388–469.
[7] D.S. Green, S.C. Wallace, J. Chem. Phys. 96 (8) (1992) 5857–5877.
[8] D. Ascenzi, S. Langford, M. Ashfold, A. Orr-Ewing, PCCP 3 (1) (2001) 29–43.
[9] Á. Logadóttir, Á. Kvaran, H. Wang, J. Chem. Phys. 109 (14) (1998) 5856–5867.
[10] Á. Logadóttir, Á. Kvaran, H. Wang, J. Chem. Phys. 112 (24) (2000) 10811–10820.
[11] Á. Kvaran, H. Wang, J. Mol. Spectrosc. 228 (1) (2004) 143–151.
[12] K. Matthiasson, Á. Kvaran, H. Wang, A. Bodi, E. Jónsson, J. Chem. Phys. 129 (17) (2008) 164313.
[13] K. Matthiasson, Á. Kvaran, H. Wang, J. Chem. Phys. 131 (4) (2009) 044324.
[14] K. Matthiasson, H. Wang, Á. Kvaran, J. Mol. Spectrosc. 255 (1) (2009) 1–5.
[15] K. Matthiasson, J. Long, H. Wang, Á. Kvaran, J. Chem. Phys. 134 (16) (2011) 164302.
[16] J. Long, H. Wang, A. Kvaran, J. Mol. Spectrosc. 282 (2012) 20–26.
[17] J. Long, H.R. Hrodmarsson, H. Wang, A. Kvaran, J. Chem. Phys 136 (2012) 214315.
[18] J. Long, H. Wang, Á. Kvaran, J. Chem. Phys. 138 (4) (2013) 044308.
[19] H.R. Hróðmarsson, H. Wang, Á. Kvaran, J. Mol. Spectrosc. 290 (2013) 5–12.
[20] H.R. Hróðmarsson, H. Wang, Á. Kvaran, J. Chem. Phys. 140 (2014) 244304.
[21] D. Zaouris, A. Kartakoullis, P. Glodic, P.C. Samartzis, H.R. Hróðmarsson, Á. Kvaran, PCCP 17 (2015) 10468–10477.
[22] P. Glodic, D. Zaouris, P.C. Samartzis, A. Hafliðason, Á. Kvaran, PCCP 18 (2016) 26291–26299.
[23] R. Callaghan, S. Arepalli, R.J. Gordon, J. Chem. Phys 86 (10) (1987) 5273–5280.
[24] J.A. Coxon, P.G. Hajigeorgiou, K.P. Huber, J. Mol. Spectrosc. 131 (1988) 288–300.
[25] P.J. Dagdigian, D.F. Varley, R. Liyanage, R.J. Gordon, R.W. Field, J. Chem. Phys. 105 (23) (1996) 10251–10262.
[26] H.R. Hróðmarsson, H. Wang, Á. Kvaran, J. Chem. Phys. 142 (2015) 244312.
[27] R. Callaghan, R.J. Gordon, J. Chem. Phys. 93 (1990) 4624–4636.
[28] D.S. Ginter, M.L. Ginter, S.G. Tilford, J. Mol. Spectrosc. 90 (1981) 152.
[29] Y. Xie, P.T.A. Reilly, S. Chilukuri, R.J. Gordon, J. Chem. Phys. 95 (2) (1991) 854–864.
[30] C. Romanescu, H.P. Loock, J. Chem. Phys. 127 (12) (2007) 124304.
[31] R. Liyanage, R.J. Gordon, R.W. Field, J. Chem. Phys. 109 (19) (1998) 8374–8387.
[32] H. Lefebvre-Brion, M. Salzmann, H.-W. Klausing, M. Müller, N. Böwering, U. Heinzmann, J. Phys. B 22 (1989) 3891.
[33] H. Lefebvre-Brion, F. Keller, J. Chem. Phys. 90 (12) (1989) 7176–7183.
[34] A.J. Yencha, D. Kaur, R.J. Donovan, Á. Kvaran, A. Hopkirk, H. Lefebvre-Brion, F. Keller, J. Chem. Phys. 99 (7) (1993) 4986–4992.
[35] S.G. Tilford, M.L. Ginter, J. Mol. Spectrosc. 40 (1971) 568–579.
[36] J.A. Coxon, U.K. Roychowdhury, Can. J. Phys. 63 (1985) 1485–1497.
[37] R.F. Barrow, J.G. Stamper, Proc. Roy. Soc. Ser. A. 263 (1961) 259–276.
[38] J. Nee, M. Suto, L. Lee, J. Phys. B: At. Mol. Phys. 18 (1985) L293–L294.
[39] J.B. Nee, M. Suto, L.C. Lee, J. Chem. Phys. 85 (1986) 719–724.
[40] J.B. Nee, M. Suto, L.C. Lee, J. Chem. Phys. 85 (1986) 4919.
[41] T.A. Spiglanin, D.W. Chandler, D.H. Parker, Chem. Phys. Lett. 137 (5) (1987) 414–420.
[42] E.d. Beer, W.J. Buma, C.A.d. Lange, J. Chem. Phys. 99(5) (1993) 3252–3261.

[43] B.G. Waage, Á. Kvaran, H. Wang, J. Chem. Phys. 113 (5) (2000) 1755–1761.
[44] H.R. Hróðmarsson, A. Kartakoullis, D. Zaouris, P. Glodic, H. Wang, P.C. Samartzis, Á. Kvaran, PCCP 19 (18) (2017) 11354–11365.
[45] S. Kauczok, C. Maul, A.I. Chichinin, K.H. Gericke, J. Chem. Phys. 133 (2) (2010) 24301.
[46] S. Manzhos, C. Romanescu, H.P. Loock, J.G. Underwood, J. Chem. Phys 121 (23) (2004) 11802–11809.
[47] C. Romanescu, H.-P. Loock, PCCP 8 (25) (2006) 2940–2949.
[48] H. Lefebvre-Brion, H.P. Liebermann, G.J. Vázquez, J. Chem. Phys. 134 (2011) 204104.
[49] S. Engin, N. Sisourat, S. Carniato, J. Chem. Phys. 137 (2012) 154304.
[50] D.M. Hirst, M.F. Guest, Mol. Phys. 41 (6) (1980) 1483–1491.
[51] W.J. Stevens, M. Krauss, J. Chem. Phys. 77 (1982) 1368–1372.
[52] M. Bettendorff, R.J. Buenker, S.D. Peyerimhoff, J. Romelt, Z. Phys. a-Hadrons Nuclei 304 (2) (1982) 125–135.
[53] Y. Li, O. Bludsky, G. Hirsch, R.J. Buenker, J. Chem. Phys. 112 (1) (2000) 260–267.
[54] E. Jonsson, Ab initio REMPI Spectra of HCl and HF, Chemistry, University of Iceland, Reykjavik, 2008.
[55] E.F.v. Dishoeck, M.C.v. Hemert, A. Dalgarno, J. Chem. Phys. 77(7) (1982) 3693–3702.
[56] M. Bettendorff, S.D. Peyerimhoff, R.J. Buenker, Chem. Phys. 66 (1982) 261–279.
[57] E.d. Beer, B.G. Koenders, M.P. Koopmans, C.A.d. Lange, J. Chem. Soc. Faraday Trans. 86(11) (1990) 2035–2041.
[58] Á. Kvaran, H. Wang, Mol. Phys. 100 (22) (2002) 3513–3519.
[59] D.P. Shoemaker, C.W. Garland, J.W. Nibler, Experiments in Physical Chemistry, fifth ed., McGraw-Hill Book Company, 1989.
[60] W. Huasheng, J. Ásgeirsson, Á. Kvaran, R.J. Donovan, R.V. Flood, K.P. Lawley, T. Ridley, A.J. Yencha, J. Mol. Struct. 293 (1993) 217–222.
[61] Á. Kvaran, H. Wang, J. Ásgeirsson, J. Mol. Spectrosc. 163 (1994) 541–558.
[62] a.D. See supplementary material, for REMPI spectra and tables of rotational lines for Rydberg states and ion-pair states of DCl.
[63] C.M. Western, PGOPHER, a Program for Simulating Rotational Structure, C. M. Western, University of Bristol, 9.0.116 ed., University of Bristol 2003-2015. <http://pgopher.chm.bris.ac.uk>.
[64] "Constants of diatomic molecules", NIST Chemistry WebBook. <http://webbook.nist.gov/cgi/cbook.cgi?ID=C7698057&Units=SI&Mask=1000> (accessed May 2017).
[65] H.R. Hróðmarsson, 2D-REMPI of HBr: Study of Singlet and Triplet Rydberg States and the Ion-pair State, Chemistry, BS, University of Iceland, Reykjavik, 2011.
[66] G.H. Jóhannesson, H. Wang, Á. Kvaran, J. Mol. Spectrosc. 179 (1996) 334–341.
[67] Á. Kvaran, H. Wang, G.H. Jóhannesson, J. Phys. Chem. 99 (13) (1995) 4451–4457.
[68] G. Herzberg, Molecular Spectra and Molecular Structure; I. Spectra of Diatomic Molecules, second ed., Van Nostrand Reinhold Company, New York, 1950.
[69] C. Romanescu, S. Manzhos, D. Boldovsky, J. Clarke, H. Loock, J. Chem. Phys 120 (2) (2004) 767–777.
[70] A.I. Chichinin, C. Maul, K.H. Gericke, J. Chem. Phys. 124 (22) (2006) 224324.